

An HTS Narrow Bandwidth Coplanar Shunt Inductively Coupled Microwave Bandpass Filter on LaAlO_3

Andreas Vogt and Wilhelm Jutzi, *Senior Member, IEEE*

Abstract— Coplanar waveguide bandpass filters with shunt inductively coupled resonators using high-temperature superconductors (HTS's) on LaAlO_3 substrates were developed for high packing density, narrow bandwidth, and low power applications. The computer-aided design and measurements on resonators to test weak end-coupling are described in this paper. A coplanar three-pole Chebychev bandpass filter with 1.8% 3-dB bandwidth at 10 GHz and 1.3-dB insertion loss at 77 K was fabricated and measured. The maximum superconducting current density of the filter is evaluated.

Index Terms— Superconducting filters.

I. INTRODUCTION

HIGH-PERFORMANCE planar microwave filter circuits are feasible with high-temperature superconductors (HTS's) thin films. The surface resistance of the ceramic superconductor $\text{YBa}_2\text{Cu}_3\text{O}_{7-8}$ (YBCO) is about a hundred times lower at microwave frequencies than the best normal conducting copper material. Therefore, the conductor area of filter circuits with these materials could be miniaturized by this factor for comparable performance. Small-size low-loss superconducting microstrip lines can be mounted on the coldfinger of a readily available closed-cycle stirling machine [1], for example. Superconducting filters for satellite communication [2] and cellular base-stations [3] have been proposed.

Filters with capacitively coupled parallel microstrips [4] as shown in Fig. 1(bottom) are often used to get a bandpass characteristic. Broadband filter performance can be designed with commercial programs. However, filters with the desired low insertion loss (<1 dB) and narrow bandwidth (0.5%–3%) on substrates for HTS's with a large dielectric constant like LaAlO_3 ($\epsilon_r = 23.8$) are difficult to synthesize with existing computer programs and require a precision implementation. Electromagnetic-field simulations are needed [5]. For a 3-dB bandwidth of 1.8% the separation between the parallel-strip quarter-wavelength sections is about four times the substrate thickness. Capacitively end-coupled microstrip filters on large dielectric constant substrates require large separations to implement small capacitive coupling for a small bandwidth. Therefore, the capacitively coupled microstrip filter area is

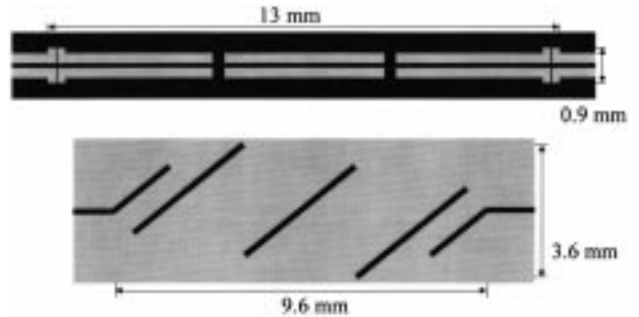


Fig. 1. Layout of two three-pole Chebychev bandpass filters of 1.8% 3-dB bandwidth at 10 GHz on LaAlO_3 , $\epsilon_r = 23.8$, implemented as (top) shunt inductively coupled coplanar waveguide (filter area $13 \times 0.9 \text{ mm}^2 = 11.7 \text{ mm}^2$) and (bottom) microstrip ($9.6 \times 3.6 \text{ mm}^2 = 34.6 \text{ mm}^2$).

rather large. Moreover, coupling beyond the adjacent resonators sections must be taken into account and hamper a straightforward design. Variations of the substrate thickness may also limit the performance of microstrip filters.

Narrow bandwidth with inductively end-coupled coplanar resonators can be implemented within a smaller area than with capacitively coupled microstrip lines. The resonators must have high quality factors. For example, a nine-pole Chebychev bandpass filter of 0.2% 3-dB bandwidth with an insertion loss of 0.8 dB requires an unloaded quality factor $Q_o = 10000$. Moderate-bandwidth filters with capacitively end-coupled coplanar waveguides have been investigated in [6]. Coplanar waveguides (CPW) with normal conductors where the resonators were coupled via inductive shunts were investigated in [7]. A strong miniaturization of coplanar stripline filters with low insertion loss and narrow bandwidth is possible with superconductors. An HTS inductively end-coupled CPW bandpass filter with a moderate bandwidth of 7.5% at 35 GHz and lateral offsets between the resonators is described in [8]. It is difficult to realize sufficiently small shunt inductances at 35 GHz and sufficiently large inductances at 10 GHz.

The layout of a shunt inductively coupled coplanar waveguide three-pole Chebychev bandpass filter on LaAlO_3 of a 1.8% 3-dB bandwidth at 10 GHz is shown in Fig. 1(top). The three resonators are shorted by four symmetric shunt inductances. A small inductance value implemented with a broad strip between inner and outer connectors yields a weak coupling between neighboring resonators. Large inductances with narrow strips and large gaps between inner and outer

Manuscript received August 12, 1996; revised December 9, 1996.

The authors are with the Institut für Elektrotechnische Grundlagen der Informatik, University of Karlsruhe, D-76187 Karlsruhe, Germany.

Publisher Item Identifier S 0018-9480(97)02538-6.

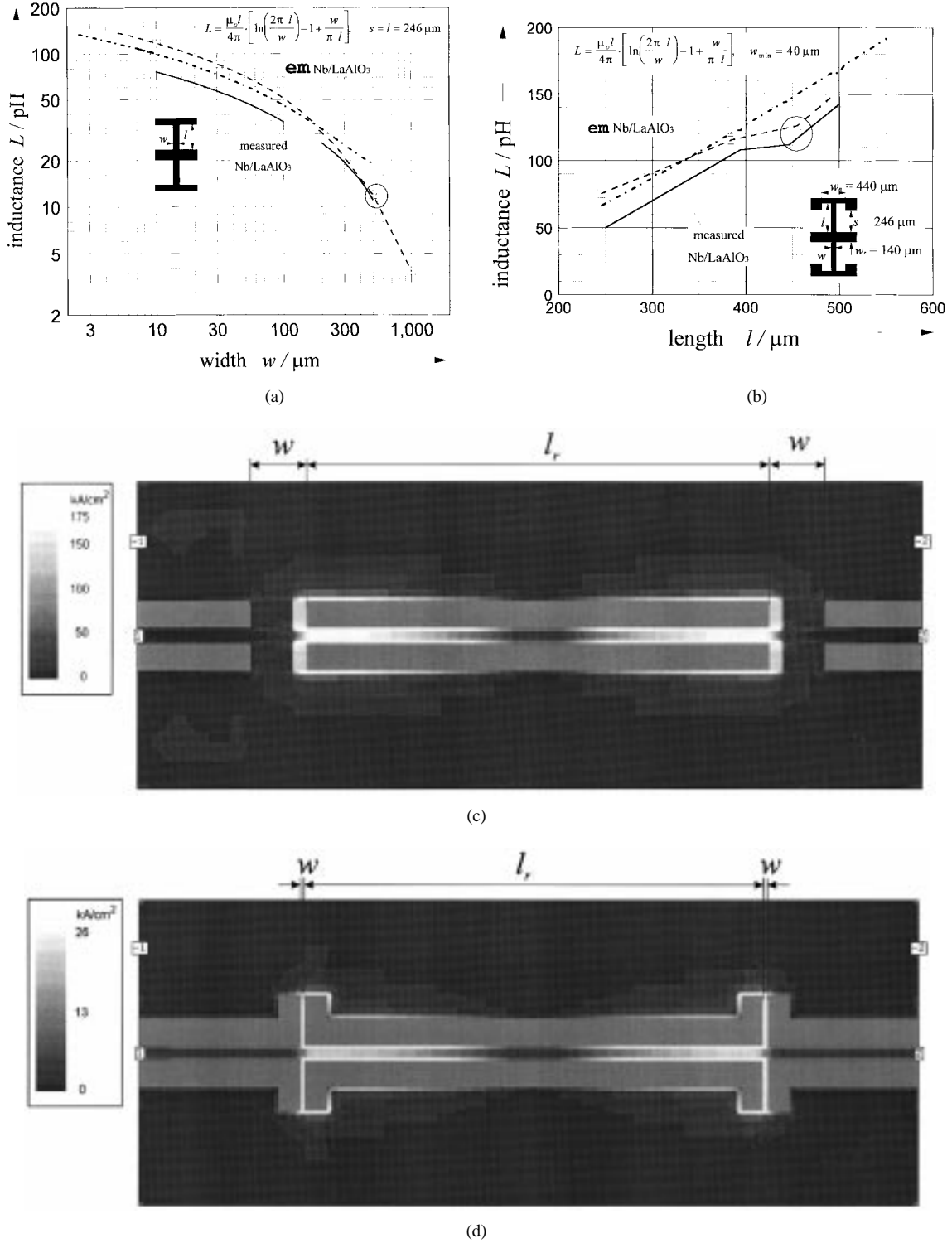


Fig. 2. Shunt inductance L as a function of the width w and (a) length l and (b) of Nb test structures calculated with the **em**-program of SONNET (-□-), the analytical formula (---), and measured results with Nb (-○-). Layout and the calculated current density distribution for a minimum discretization $\Delta x = 40 \mu\text{m}$ (gray shaded, $p_1 = 0 \text{ dBm}$, $\lambda_L = 365 \text{ nm}$) of a test resonator with $t = 600\text{-nm}$ thick YBCO films on a 0.5-mm LaAlO_3 substrate, (c) weakly coupled $l_r = 4.14 \text{ mm}$, $w_r = 140 \mu\text{m}$, $w = 500 \mu\text{m}$, $s = l = 246 \mu\text{m}$, (d) strongly coupled $l_r = 4.14 \text{ mm}$, $w_r = 140 \mu\text{m}$, $s = 246 \mu\text{m}$, $w = 500 \mu\text{m}$, $l = 455 \mu\text{m}$, $w_n = 440 \mu\text{m}$. The circles represent the geometries (c) and (d).

conductors were implemented for the two outer shorts in Fig. 1(top). The length of the shorts between the resonators is small compared with the wavelength. The dimensions of the coplanar shorts are considerably smaller than the separation of the edge-coupled microstrip resonators in Fig. 1(bottom). Since

the coupling between the next coplanar resonator section may be neglected, the CPW design is simpler. Coplanar structures are very well suited to integration of complex filters and semiconductor circuits at reasonable cost. The dimensions of *short-circuited* inductively end-coupled microstrip filters

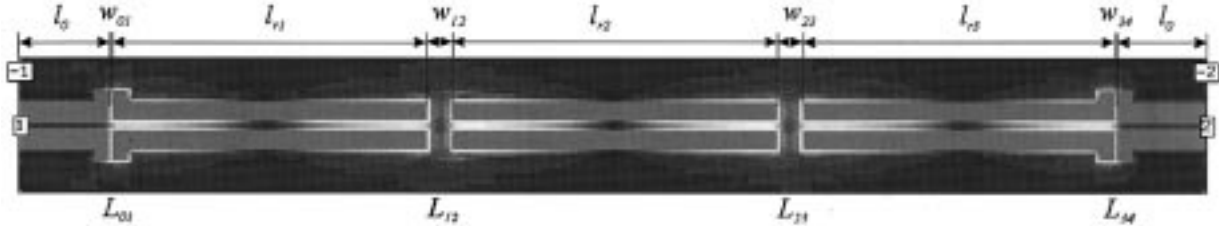


Fig. 3. Layout and calculated current density distribution for a minimum discretization $\Delta x = 40 \mu\text{m}$ (gray shaded, $j_{\max} = 96 \text{ kA/cm}^2$ for $p_1 = 0 \text{ dBm}$, $T = 77 \text{ K}$, $\lambda_L = 365 \text{ nm}$) of a 3-dB $BW/f_o = 1.8\%$ three-pole Chebychev coplanar waveguide bandpass filter at $f_o = 10.06 \text{ GHz}$. The total length is $2(w_{01} + l_{r1} + w_{12}) + l_{r2} = 12.7 \text{ mm}$, the orthogonal dimension of the shorts is 0.9 mm .

could be of the same order as the CPW solution. Since superconducting vias between the microstrip and the ground plane through LaAlO_3 are very difficult to implement with the present technology, these types of filters are no longer considered in this paper.

II. FILTER DESIGN

The filter parameters have been determined via a transformation of a low-pass prototype in a bandpass between $Z_o = 50 \Omega$ terminals [9]. The inductively end-coupled bandpass filter comprises half-wave resonators, symmetric shunt inductors, and about $\lambda/4$ impedance transformers at output and input [7]. The resonator characteristic impedances were chosen to be $Z_{o,r} = Z_o = 50 \Omega$. The coupling inductance L is given by the equation:

$$\frac{Z_o}{2\pi f_o L} = \frac{Z_o}{K} - \frac{K}{Z_o} \quad (1)$$

where f_o and K are the filter center frequency and the coupling coefficient of the impedance (K) inverter. In a first approach for ideal conductors the inductance length of a single strip between two coplanar conducting half-planes with the length l and the width w has been approximated [7]:

$$L_s \approx \frac{\mu_{0l}}{2\pi} \left[\ln \left(\frac{2\pi l}{w} \right) - 1 + \frac{w}{\pi l} \right]. \quad (2)$$

The corresponding calculated inductance of two such strips in parallel between the inner conductor and the ground of the coplanar waveguide versus w and l are represented in Fig. 2(a) and (b), respectively, as a dash-dotted line. Weak coupling, $K/Z_o \cong 0.03$ for narrow-bandwidth is obtained for $w/l \cong 1$. In order to check the approximation formula Nb-resonators have been simulated with the electromagnetic full-wave analysis program **em** SONNET [10] and plotted as a dashed line in Fig. 2(a). The properties of the 200-nm-thick Nb films on 0.5-nm thick LaAlO_3 substrates have been specified by the surface resistance at 10 GHz and a constant (dc) surface *kinetic* inductance $\mu_o \lambda_L$, where λ_L is the London penetration depth. The measured effective coupling inductance as obtained by the loaded quality factor and center frequency of the simulated S -parameter response, is represented in Fig. 2(a) by a continuous line.

The layout of a weakly and strongly coupled resonator with 600-nm-thick YBCO films on 0.5-nm-thick LaAlO_3 and the corresponding current density distribution at resonance frequency, calculated with the **em** program, are displayed in Fig.

2(c) and (d). Since the minimum discretization $\Delta = 35 \mu\text{m}$ has been chosen much larger than the London penetration depth to reduce the requirement of computer memory and time, the current densities are expected to be an order of magnitude too small; however, the calculated inductances seem to match the measured results. The results of the **em** program mentioned in the following are used to compare different structures with the same mentioned minimum discretization and input power. If one dimension is smaller than $35 \mu\text{m}$ as the width w in Fig. 2(a), it is approximated $w = \Delta$. The peak current densities occur at the rectangular corner of the shunt inductances and the inner conductor of the coplanar waveguide in Fig. 2(c) are $j_{\max} \geq 450 \text{ kA/cm}^2$ for $\lambda_L = 365 \text{ nm}$ (YBCO, 77 K) at 0-dBm input power corresponding to a loaded quality factor $Q_L = 2760$. In Fig. 2(d) the maximum is within the shunt strip and has the value 60 kA/cm^2 at 0 dBm. The quality factor $Q_L = 33$ is much smaller than in Fig. 2(c) owing to larger coupling inductances and, hence, stronger loading via the 50Ω input and output lines. As expected, the maximum current density is larger for larger quality factors. In Fig. 2(d) the shunt inductor length is larger than the gaps in order to get a larger inductance at a minimum linewidth w_{\min} of the inner shunt conductor.

To verify the calculations by measurements Niobium test resonators on LaAlO_3 substrates were fabricated first. Two hundred-nm-thick sputtered Nb was deposited on one side of a LaAlO_3 substrate. The inner conductor width was $w_r = 140 \mu\text{m}$, the gap width $s = 246 \mu\text{m}$ and the resonator length $l_r = 4.14 \text{ mm}$, with a characteristic impedance $Z_o = 50 \Omega$ and a center frequency $f_o = 10 \text{ GHz}$. Aluminum bridges equidistantly bonded between the two ground conductors suppressed slotline modes. The center frequency, the loaded quality factor Q_L , and the transmission coefficient $|S_{21}|$ near f_o at $T = 4.2 \text{ K}$ in helium gas were measured with a vector network analyzer. The normalized coupling coefficients were calculated with [9]

$$\frac{K}{Z_o} = \sqrt{\frac{\pi}{4} \frac{|S_{21}|}{Q_L}}. \quad (3)$$

The measured unloaded quality factors of these resonators with $s = l = 246 \mu\text{m}$ reached $Q_o \geq 10000$ for the weakest couplings ($w = 1 \text{ mm}$, $K/Z_o = 0.004$). The dielectric losses ($\tan \delta \cong 8 \cdot 10^{-6}$ at 77 K [11]) of LaAlO_3 and conductor losses ($R_s = 20 \mu\Omega$, 10 GHz, 4.2 K [12]) of Niobium should be almost negligible. The unloaded quality factor of the shorted resonator is mainly limited by radiation losses,

TABLE I
FILTER SPECIFICATION: THREE-POLE CHEBYCHEV

center frequency	10.0 GHz
ripple	0.2 dB
3-dB bandwidth	120 MHz
insertion loss	< 0.1 dB

which can be further decreased by reducing the gap width s of the coplanar waveguide. Note, that an open resonator would have more than two times higher radiation losses. The measured shunt inductances have been within 80% of the calculated values according to (2) for strong couplings ($17\ \mu\text{m} < w < 100\ \mu\text{m}$) and within 67% of the **em**-simulation. The disagreement between the **em**-simulation and the measurement of the inductances is not yet fully understood. The influence of SMA-coplanar transitions, box and slotline modes on strongly coupled resonators must be further investigated. For weakly coupled structures ($w > 100\ \mu\text{m}$) the agreement between the results of **em**-simulation with $\Delta/w \ll 1$ and measurement improves, where the approximation (2) yields bad results. Fortunately enough, the required inductances are in the ranges, where the agreement is rather satisfactory (see circles).

The measured coupling coefficients have been used as guidelines to start the design of narrow-bandwidth filter in the X-band, shown in Table I.

The corresponding coupling coefficients $K_{01}/Z_o = 0.11$ and $K_{12}/Z_o = 0.013$ [7] yield the inductances $L_{01} = 91\ \text{pH}$ and $L_{12} = 11\ \text{pH}$. L_{01} and L_{12} were implemented with the geometric parameters $w_{01} = w_{\min} = 40\ \mu\text{m}$, $l_{01} = 407\ \mu\text{m} > s = 246\ \mu\text{m}$, $w_n = 440\ \mu\text{m}$ and $w_{12} = 314\ \mu\text{m}$, $l_{12} = 246\ \mu\text{m} = s$, respectively. The measurements of the inductances in Fig. 2(a) and (b) were done partly after the final filter design, so the extrapolated geometries $l_{01} = 407\ \mu\text{m}$ and $w_{12} = 314\ \mu\text{m}$ for L_{01} and L_{12} were used. According to Fig. 2(a) and (b), these structures yield too high inductances $L_{01} = 110\ \text{pH}$ and $L_{12} = 19\ \text{pH}$. However, the filter was realized with this geometry. Sufficiently small shunt inductances can be achieved. Smaller characteristic impedances of the resonator sections than $50\ \Omega$ and offset transmission lines [8] are not needed here. Moreover, smaller resonator characteristic impedances are avoided as they lead to higher current densities.

At 10 GHz a surface resistance of 600-nm-thick YBCO films $R_s(77\ \text{K}) = 375\ \mu\Omega$ has been assumed and a wavelength on the YBCO line (London penetration depth $\lambda_L(77\ \text{K}) = 365\ \text{nm}$) with a LaAlO_3 substrate ($\epsilon_r(77\ \text{K}) = 23.8$) $\lambda = 8.28\ \text{mm}$ has been calculated. The kinetic inductance decreases the propagation velocity and wavelength of this YBCO line compared to ideal conductors with 5%. The corresponding layout and the **em**-calculated current density distribution (gray scaled) are shown in Fig. 3. The input power level 0 dBm was chosen to easily compare the results with a common standard.

A SPICE simulation with lumped shunts L_{ik} and distributed lossy transmission lines with $l_{r1} = l_{r3} = 3974\ \mu\text{m}$, $l_{r2} = 4105\ \mu\text{m}$ and $R' = 0.012R_s/\mu\text{m} = 4.5\ \mu\Omega/\mu\text{m}$, $L' = 604\ \text{fH}/\mu\text{m}$, $C' = 242\ \text{aF}/\mu\text{m}$ [13] neglecting radiation coupling yields a good agreement with the design goals of 120-MHz 3-dB bandwidth. The simulated insertion loss was $IL = 0.2\ \text{dB}$.

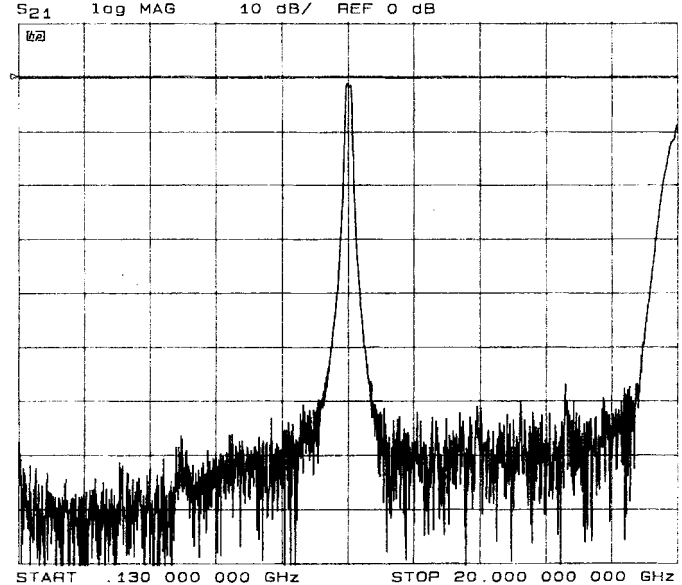


Fig. 4. Measured $|\underline{S}_{21}|$ -parameter as a function of frequency of a three-pole Chebychev YBCO coplanar waveguide bandpass filter with a $3\ \text{dB}\ BW/f_o = 1.8\%$ at $f_o = 10\ \text{GHz}$ on LaAlO_3 and at $T = 77\ \text{K}$ according to Fig. 3.

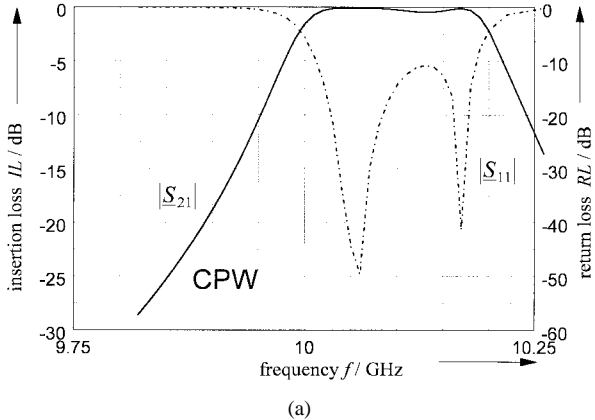
III. FILTER FABRICATION AND MEASUREMENT

C-axis-oriented thin films of the high-temperature superconductor $\text{YBa}_2\text{Cu}_3\text{O}_7 - \delta$ have been grown by off-axis sputtering from a stoichiometric target on polished LaAlO_3 substrates [14]. The critical temperature and critical current density of superconductivity has been measured as $T_c = 89\ \text{K}$, $j_c(77\ \text{K}) = 3 \cdot 10^6\ \text{A}/\text{cm}^2$. A 50-nm gold layer was thermally evaporated on the 600-nm thick YBCO film in certain areas for low-ohmic-resistive contacts for aluminum bond bridges between the coplanar grounds, at coplanar to coaxial connectors and for trimming of the shunts. The gold film partly covered the shunt inductors in order to trim the filter properties by piecewise removing of the normal conducting layer.

The structures were patterned by argon ion-beam etching. The filter was mounted in a gold-plated brass housing with inner dimensions $17 \times 5 \times 6\ \text{mm}^3$ and SMA connectors. No absorbing sheets are introduced to attenuate unwanted box resonances. The coplanar ground contacts with the housing were reinforced with indium-wires and silver paste.

The \underline{S} -parameter measurements have been performed with a vector network analyzer. The filter package was placed inside a cold helium-gas cryostat via flexible cable and stainless-steel semirigid cable with an overall length of 7 m. At $T = 77\ \text{K}$ an insertion loss calibration comprising a $50\text{-}\Omega$ superconducting coplanar waveguide of the overall filter length and SMA connectors and a short-circuit reflection calibration at the end of the input SMA connector without CPW have been performed.

The measured $|\underline{S}_{21}|$ -parameter as a function of frequency up to 20 GHz of the three-pole CPW bandpass filter at $f_o = 10\ \text{GHz}$ and $T = 77\ \text{K}$ on LaAlO_3 is plotted in Fig. 4. In the whole frequency area the filter performance is disturbed neither by slotline modes nor box resonances. No couplings between the next resonator section seems to occur. The filter



(a)

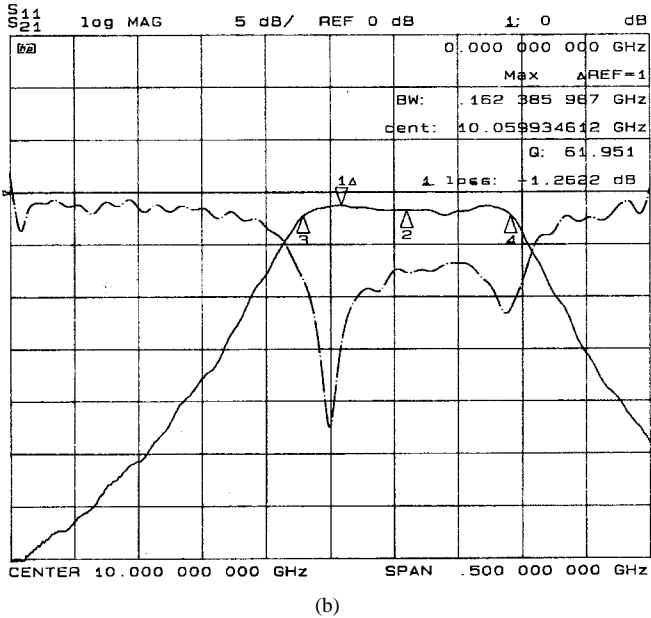


Fig. 5. (a) The **em**-calculation by SONNET of $|\underline{S}|$ -parameters in the passband of a 3-dB $BW/f_o = 1.8\%$ three-pole Chebychev YBCO coplanar waveguide bandpass filter at $f_o = 10.06$ GHz on LaAlO_3 and (b) the measured results at $T = 77$ K.

roll-offs are nearly symmetric to the center frequency. The frequency slope of the left and right side is 16 MHz/3 dB and 15 MHz/3 dB, respectively, which is in good agreement with 12 MHz/3 dB, the value of the design tables [9]. The maximum output power of the network analyzer $p_o = -10$ dBm has been increased with an external amplifier by 25 dB; no degradation of the filter bandwidth and passband flatness has been observed.

The **em**-calculation of the filter layout in Fig. 3 exhibited a 3-dB bandwidth $BW = 190$ MHz, which is larger than the mentioned 120 MHz of SPICE simulation with inductive shunts and lossy transmission lines. The measured results and the **em**-calculation of the $|\underline{S}|$ -parameters as a function of the frequency in the passband at 10 GHz are compared in Fig. 5(a) and (b), and shown in Table II.

After trimming the input inductors by removing gold or adding dots of indium, a flat filter passband was achieved. The measured insertion loss $IL = 1.3$ dB was higher than $IL < 0.1$ dB, the calculated value with the **em**-program

TABLE II

	em-calculation	measurement
center frequency	10.1 GHz	10.06 GHz
ripple	0.5 dB	1.0 dB
fractional		
3 dB bandwidth	1.9%	1.8%
insertion loss	< 0.1 dB	1.3 dB
return loss	> 6 dB	> 7 dB

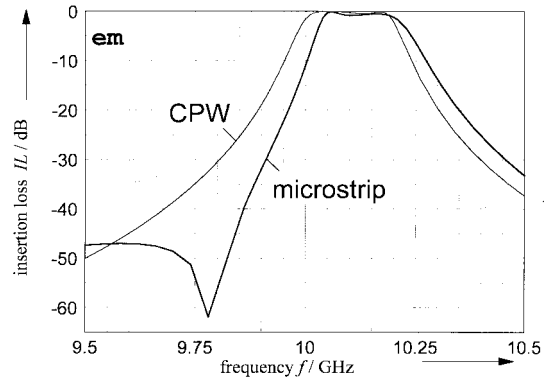


Fig. 6. The **em**-calculation of $|\underline{S}|$ -parameters in the passband of 3-dB $BW/f_o = 1.9\%$ three-pole Chebychev YBCO microstrip and CPW bandpass filters on LaAlO_3 .

for YBCO films ($R_s(77$ K, 10 GHz) = $375 \mu\Omega$, $t > \lambda_L$). The above measurement was calibrated with a 50Ω coplanar waveguide having the same cross-sectional geometry and the same male and female SMA connectors as the filter. This coplanar waveguide yielded $IL = 1$ dB as calibrated with only female and male SMA connectors. So the measured insertion loss seems to be quite sensitive to the adjustment of the coaxial SMA-CPW transition. The return loss measurement of S_{11} is plotted in Fig. 5(a) and (b) as a dash-dotted line. It has been measured by a time-domain gate, filtering the connector reflections of the long interconnection cables, therefore, the frequency resolution was reduced. The measured center frequency $f_o = 10.06$ GHz and the 3-dB bandwidth $1.8\% \cdot f_o$ has been in good agreement with the **em**-calculation, although the discretization grid $\Delta x = 40 \mu\text{m}$ was rather rough compared with the stripline cross section. For a narrower bandwidth the width of the two inner shunt inductors must be increased according to Fig. 2(a).

The surface current density distribution of the filter calculated for $\Delta y = 35 \mu\text{m}$ at 10.06 GHz in Fig. 3 increases strongly near the stripline borders and at the shunts. The highest calculated values are found on the inner conductor of the coplanar waveguide at the rectangular corners of the inner resonator with the weakest coupling, but with wide inductor widths. The maximum current density in the passband is $j_{\max} \geq 96 \text{ kA/cm}^2$ for $p_1 = 0$ dBm input power and $\lambda_L(77\text{K}) = 365 \text{ nm}$. In comparison, a three-pole microstrip bandpass filter has been designed and simulated with the **em**-program. The thickness of the LaAlO_3 substrate was $h = 0.5$ mm, the strip width $w = 160 \mu\text{m}$. A layout according to Fig. 1(bottom) has been used. The simulated insertion loss versus the frequency is plotted in Fig. 6. The passband ripple has not yet been optimized. The calculated maximum current density

with a minimum discretization $\Delta = 40 \mu\text{m}$ for $p_1 = 0 \text{ dBm}$ is $j_{\max} \leq 88 \text{ kA/cm}^2$ at the inner YBCO resonator and only about 9% smaller than that of a CPW filter having comparable bandpass characteristics. The calculated maximum current density ratio at the chosen cross sections of microstrip and CPW stays essentially constant if the minimum discretization is reduced below the London penetration depth.

IV. CONCLUSION

Design and measurement of compact narrow-bandwidth shunt inductively coupled coplanar waveguide bandpass filters with $\text{Y}_1\text{Ba}_2\text{Cu}_3\text{O}_7 - \delta$ films on LaAlO_3 substrates at 77 K has been described. The filter design has been aided by an electromagnetic wave analysis program. SONNET calculations and measurements have been in good agreement. A three-pole Chebychev bandpass filter at 10.06-GHz 1.3-dB insertion loss, and 1.8% 3-dB bandwidth for a receiver filterbank has been achieved. For comparable bandpass characteristic (50- Ω -line, bandwidth, roll-off, center frequency) the coplanar waveguide structure requires less than half the surface area at the expense of only 9% larger maximum current density than the microstrip structure. The design and trimming of CPW filters is simplified as radiation coupling between resonators is very small. The measured insertion losses can probably be decreased with an improved coaxial to coplanar waveguide transition.

ACKNOWLEDGMENT

The authors wish to thank Dr. M. Neuhaus and Dr. T. Scherer for sputtering Nb and YBCO films and Dr. R. Herwig for ion etching the structures. The numerical work of G. Benz is greatly appreciated. The skillful preparation and bonding of chips by A. Stassen and H.-J. Wermund has been essential for the successful measurements.

REFERENCES

- [1] Daimler-Benz Industrie, AEG, Theresienstr. 2, D-74072 Heilbronn/Germany, 2-W-Linear-Split-Cycle-Stirling cooler.
- [2] G. W. Mitschang, "Space applications and implications of high temperature superconductivity," *IEEE Trans. Appl. Superconduct.*, vol. 5, pp. 69-73, June 1995.
- [3] G.-C. Liang, D. Zhang, C.-F. Shih, M. E. Johansson, R. S. Withers, A. C. Anderson, and D. E. Oates, "High-power high-temperature superconducting microstrip filters for cellular base-station applications," *IEEE Trans. Appl. Superconduct.*, vol. 5, pp. 2652-2655, June 1995.
- [4] S. H. Talisa, M. A. Janocko, D. L. Meier, C. Moskowitz, R. L. Grassel, J. Talvacchio, P. LePage, G. Hira, D. C. Buck, S. J. Pieseski, J. C. Brown, and G. R. Wagner, "High-temperature superconducting four-channel filterbanks," *IEEE Trans. Appl. Superconduct.*, vol. 5, pp. 2079-2082, June 1995.
- [5] J. W. Chandler, R. M. Biernacki, S. H. Chen, W. J. Getsinger, P. J. Grobelny, C. Moskowitz, and S. T. Talisa, "Electromagnetic design of

high-temperature superconducting microwave filters," *Int. J. Microwave and Millimeter-Wave Comput.-Aided Eng.*, vol. 5, pp. 331-343, 1995.

- [6] D. F. Williams and S. E. Schwarz, "Design and performance of coplanar waveguide bandpass filters," *IEEE Trans. Microwave Theory Tech.*, vol. MTT-31, no. 7, pp. 558-566, July 1983.
- [7] J. K. A. Everad and K. K. M. Cheng, "High performance direct coupled bandpass filters on coplanar waveguide," *IEEE Trans. Microwave Theory Tech.*, vol. 41, pp. 1568-1573, Sept. 1993.
- [8] D. G. Swanson, Jr. and R. J. Forse, "An HTS end-coupled CPW filter at 35 GHz," in *IEEE Microwave Theory and Tech. Symp. Dig.*, May 1994, vol. 1, pp. 199-202.
- [9] G. L. Matthei, L. Young, and E. M. T. Jones, *Microwave Filters, Impedance-Matching Networks and Coupling Structures*. New York: McGraw-Hill, 1964.
- [10] *em User's Manual and xgeom User's Manual*, Liverpool, NY: Sonnet Software, Inc., 1994.
- [11] J. Krupka, R. G. Geyer, M. Kuhn, and J. Hinken, "Dielectric properties of single crystals of Al_2O_3 , LaAlO_3 , NdGaO_3 , SrTiO_3 and MgO at cryogenics temperatures," *IEEE Trans. Microwave Theory Tech.*, vol. 42, pp. 1886-1890, Oct. 1994.
- [12] A. Vogt, R. Herwig, P. Marienhoff, M. Neuhaus, T. Scherer, and W. Jutzi, "Microwave surface resonances with partially untwinned YBCO films near 10 GHz," *IEEE Trans. Appl. Superconduct.*, vol. 3, pp. 1715-1718, Mar. 1993.
- [13] R. K. Hoffmann, *Integrierte Mikrowellen Schaltungen*. Berlin, Germany: Springer-Verlag, 1983.
- [14] T. Scherer, R. Herwig, P. Marienhoff, M. Neuhaus, A. Vogt, and W. Jutzi, "Off-axis sputtered $\text{YBa}_2\text{Cu}_3\text{O}_{7-\delta}$ films on NdGaO_3 ," *Cryogenics*, vol. 31, pp. 975-978, Nov. 1991.



Andreas Vogt was born in Heilbronn at the Neckar River, Germany. He received the MS (Dipl.-Ing.) degree in electrical engineering from the University of Karlsruhe, Karlsruhe, Germany, in 1990, working on "Chip floorplanning with neural networks."

In July 1990 he joined the Institut für Elektrotechnische Grundlagen der Informatik, University of Karlsruhe and designed, simulated, and measured microwave devices of high-temperature superconductors.



Wilhelm Jutzi (SM'91) received the MS (Dipl.-Ing.) and Ph.D. (Dr.-Ing.) degrees from the Technische Hochschule Darmstadt, Germany, in 1958 and 1962, respectively.

He joined Zürich IBM Research Laboratory in 1961 and worked on striplines, fast digital memory cells with thin magnetic films, Si- and GaAs-MESFET's, and digital circuits with Josephson junctions. Since 1975 he has been Head of the Institut für Elektrotechnische Grundlagen der Informatik at the University of Karlsruhe, Karlsruhe, Germany. From 1988 to 1990 he was Dean of the faculty of electrical engineering at the University of Karlsruhe. He has lectured on various subjects, including digital circuits, digital memories and semi- and superconductor integrated circuits. His research activities are concentrated on the conception, simulation, fabrication, and measurements of fast integrated digital and microwave circuits with metallic and oxide superconductors.

Dr. Jutzi is a member of the Informationstechnische Gesellschaft im VDE, of the Gesellschaft für Informatik, of the Deutsche Physikalische Gesellschaft.